

## Research Article

**Molecular Docking and Drug Likeness Prediction of New Potent Sars Cov-2 Main Protease Inhibitors**

EL HASSEN MOKRANI\*, SOUMIA TENIOU, RYM GOUTA DEMMAK, GUENDOUZE ASSIA, ABDELOUAHAB CHIKHI, ABDERRAHMANE BENSEGUENI

Laboratory of Applied Biochemistry, Department of Biochemistry and Cellular and Molecular Biology, Faculty of Natural and Life Sciences, University Mentouri Brothers Constantine 1. Algeria.

**ARTICLE DETAILS***Article history:*

Received on 20 May 2022

Modified on 11 June 2022

Accepted on 18 June 2022

*Keywords:*Enzyme,  
Inhibitor,  
Molecular Docking,  
M<sup>pro</sup>,  
SARS CoV-2.**ABSTRACT**

The novel corona virus whose outbreak took place in December 2019 continues to spread at a rapid rate worldwide. The Main protease (M<sup>pro</sup>) plays critical role in the SARS-CoV-2 life cycle through virus replication and transcription process making it as an attractive drug target. Herein, molecular docking study followed by drug-Likeness prediction, were performed in order to identify new potent M<sup>pro</sup> inhibitors. Indeed, molecular docking of 1880 compounds into the M<sup>pro</sup> active site reveals compounds S1 and S2 as promising inhibitors of this enzyme with binding energy of -39,22 KJ/mol, -36.27 KJ/mol respectively. These two compounds were also predicted to have satisfying drug likeness properties, indicating that they might be promising lead compounds for further anti-SARS CoV-2 drug research.

© KESS All rights reserved

**INTRODUCTION**

The corona virus disease 2019 (COVID-19) pandemic has left a mark in all countries, with more than 552 million cases worldwide and over 6.27 million deaths as of 15 Mai 2022 [1]. The clinical symptoms of COVID -19 often overlap and can affect any system in the body [2]. They include fever, sore throat dry cough, headache, pneumonia with potentially progressive respiratory failure owing to alveolar damage, and even death [3, 4].

Currently, no specific targets are available for severe acute respiratory syndrome corona virus 2 (SARS-CoV-2). However, a number of proteins are considered essential to the SARS CoV-2 lifecycle and therefore provide a significant number of targets for inhibiting viral host entry and replication [5]. Indeed, during viral replication, the SARS CoV-2 Main protease (M<sup>pro</sup>) plays crucial role in the viral life cycle through virus replication and transcription process. Hence, this enzyme presents attractive targets for small molecule inhibitors since no human proteases with a similar specified cleavage are characterized [6].

Thus, the identification of new potent M<sup>pro</sup> inhibitors with improved pharmacokinetic properties remains important.

Herein, molecular docking approach followed by visual inspection and drug likeness prediction were performed in order to identify new potent SARS CoV-2 M<sup>pro</sup> inhibitors, which could help in progressive attempts in the therapeutics of COVID-19

**MATERIALS AND METHODS****Protein Preparation**

The crystal structure of SARS-CoV-2 main protease (M<sup>pro</sup>) in complex with **S-[5-(TRIFLUOROMETHYL)-4H-1,2,4-TRIAZOL-3-YL] 5-(PHENYLETHYNYL)FURAN-2-CARBOTHIOATE (F3F); a potent inhibitor, was retrieved** from the Protein Data Bank (PDB ID: **2GZ8**) [7]. The structure of the enzyme was prepared for docking, minimized and refined using the Protein Preparation Wizard implemented in Schrödinger suite [8]. This preparation was undertaken to eliminate crystallographic waters, to add missing hydrogen and chain atoms, and to assign the appropriate charge and protonation state for amino acid residues at pH 7.0±2. The enzyme structure was subjected to an energy minimization using the

**\*Author for Correspondence:**

Email: mohsen.mokrani@umc.edu.dz

OPLS-2005 force-field [9]. The co-crystal inhibitor (**F3E**) was used to identify the active site of M<sup>pro</sup> by selecting all amino-acids residues within a radius of 6.5 Å. This selection was refined by adding every residue beyond 6.5 Å considered as essential for the continuity of the protein cavity [10].

### Ligand Preparation

A chemical library contained 1405 analogs compounds to F3F were retrieved from PubChem database in 3D sdf format. These compounds were prepared for docking using LigPrep module of Schrödinger suite [8] which undertakes hydrogen atom addition, amending realistic bond lengths and angles and generation for each compound a number of structures with various enantiomers (when undefined), protonation states at pH 7.4±1 and tautomers. Partial charges were assigned to the structures using the OPLS-2005 force-field [11]. The final chemical library consisted of 1880 molecules in sdf format was used for docking calculations.

### Molecular Docking Calculations

Molecular docking calculations of 1880 compounds were undertaken on M<sup>pro</sup> binding site using FlexX which was based on an incremental construction of ligands. Docking calculations were done with the default parameters. FlexX scoring function, which gave scores as binding energy in kJ/mol, was used for molecule ranking [12]. FlexX requested to retain 10 poses per molecule although the ranking of a molecule was solely based on its top-ranked pose.

### Visual Inspection

The resulting top-ranked 100 compounds from docking calculation were analyzed by visual inspection in order to eliminate false positive ones. In this context, three types of interactions were considered: hydrogen bonds, π-π stacking and hydrophobic interactions. The retained molecules had to be well buried into the M<sup>pro</sup> cavity. They also had to present a good protein-ligand complementarity and an optimized number of hydrogen bonds and π-π stacking when possible, especially with the dyad catalytic residues (His41 and Cys145) [13,14].

### Validation of Docking Protocol

The Root Mean Square Deviation (RMSD) test represents the ability of a docking program to reproduce the experimental binding modes of a ligand. It is a metric, which measures average

distances between the docking binding mode and the experimental position of a ligand. The prediction is acceptable when the RMSD is less than or equal to 2 Å beyond which the prediction is considered irrelevant. In our work, the performance of the docking program FlexX was evaluated by calculating RMSD values of 100 protein-ligand crystal structures from the Protein Data Bank (PDB) [15].

### ADMET Prediction

The top ranked hits were further filtered by the prediction of their physic-chemical, pharmacokinetics and toxicity properties using ADMET lab version 2.0 (<https://admetmesh.scbdd.com>). These properties consist of Lipinski and Veber's Rule, Blood-Brain Barrier permeability (BBB), Gastro-Intestinal absorption (GI), Cytochrome P450 (CYP) inhibition, and toxicity (Ames test, hERG inhibition and carcinogenicity). The same parameters of **F3F** were also predicted for comparison.

## RESULTS AND DISCUSSIONS

### Validation of Docking Protocol

The performance of docking program (FlexX) was evaluated by calculating RMSD values of 100 protein-ligand complexes from the PDB. The predicted binding mode was considered correct when the RMSD was below 2.0 Å. As shown in Table 1, 70% of the RMSD values are less than or equal to 2 Å, thus indicating that the used docking protocol reproduce correctly the experimental conformation of a ligand in its binding site [16]. In the most cases, there was a negligible deviation between the experimental and the docked conformation as shown in Fig. 1 for M<sup>pro</sup> inhibitor (PDB ID: **2GZ8**).

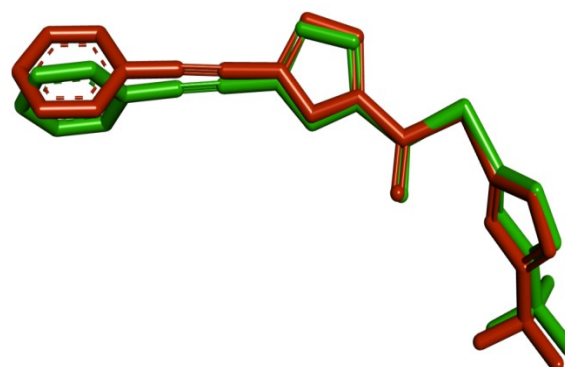


**Figure 1:** Superposition of **F3F** given by X-ray crystallography (colored in green) and by molecular docking using FlexX (colored in red).

**Table 1:** List of 100 complexes Protein-Ligand used in RMSD test.

| Protéine | Ligand | RMSD (Å) | Protéine | Ligand | RMSD (Å) | Protéine | Ligand | RMSD (Å) |
|----------|--------|----------|----------|--------|----------|----------|--------|----------|
| 1N7I     | SAH    | 1,73     | 5I3A     | HQE    | 0,36     | 2VJ8     | HA2    | 1,51     |
| 1AH3     | NAP    | 1,52     | 5TFT     | HEM    | 1,27     | 3CCC     | 7AC    | 0,76     |
| 1AIM     | ZYA    | 1,18     | 5URS     | 8LA    | 9,78     | 3I28     | 34N    | 1,29     |
| 1EB2     | BPO    | 1,5      | 5ZAN     | 9A6    | 6,05     | 3K5F     | AYH    | 1,56     |
| 1EKO     | 184    | 4,88     | 6FH5     | DD8    | 0,97     | 3K00     | 24D    | 1,8      |
| 1K1M     | FD4    | 4,41     | 6MDA     | JED    | 0,59     | 3LJT     | LA3    | 1,92     |
| 1P9S     | DIO    | 4,47     | 6MDB     | JE4    | 1,49     | 3OF8     | 10Y    | 4,95     |
| 1RTI     | HEF    | 1,96     | 6MDC     | JEA    | 1,97     | 3RZ3     | U94    | 2,43     |
| 1YKR     | 628    | 0,74     | 6MDD     | JE7    | 0,67     | 3TPP     | 5HA    | 1,45     |
| 1YZ3     | SAH    | 1,1      | 6O9X     | MOS    | 5,72     | 4CGA     | QLW    | 2,42     |
| 1ZVX     | FIN    | 1,87     | 6OA3     | MOM    | 3,7      | 4EY7     | E20    | 1,78     |
| 2G5P     | 3GP    | 3,41     | 6OHS     | MJY    | 1,62     | 4G9C     | OWP    | 1,49     |
| 2G71     | SAH    | 1,74     | 1OI9     | N20    | 0,6      | 4KZO     | NAP    | 10,02    |
| 2JBJ     | G88    | 5,3      | 2OPB     | SAH    | 1,32     | 4LXM     | 1YU    | 10,04    |
| 2ONZ     | TMJ    | 0,4      | 2QJR     | TB     | 0,84     | 4MO8     | 2VQ    | 1,94     |
| 2R4B     | GW7    | 1,3      | 3VVG     | ZGB    | 1,99     | 4OGN     | 2U5    | 1,76     |
| 2RJP     | 886    | 1,48     | 1C84     | 761    | 1,14     | 4ONC     | FMT    | 2,55     |
| 2V35     | J54    | 7,24     | 1H39     | R03    | 1,73     | 4ZZ2     | 3YG    | 1,12     |
| 2XBU     | 5GP    | 2,39     | 1LI9     | PO4    | 1,57     | 5C28     | 4XV    | 2,51     |
| 2ZJF     | BSU    | 0,48     | 1KIM     | THM    | 0,92     | 5CLU     | S8A    | 1,5      |
| 2EW8     | SO4    | 9,06     | 1N8Q     | DHB    | 1,96     | 5D0R     | B1T    | 1,18     |
| 3N9S     | TD4    | 1,19     | 1OGQ     | NAG    | 3,75     | 5EEC     | ZXN    | 1,92     |
| 3QKQ     | HEM    | 1,21     | 1PNN     | 984    | 1,45     | 5HVT     | NVS    | 1,15     |
| 3QTQ     | X35    | 0,67     | 1YW8     | A75    | 2,8      | 5IWC     | 6EQ    | 2,31     |
| 3VP2     | BP0    | 1,84     | 2AN5     | SAH    | 1,18     | 5J9Y     | 6HL    | 1,95     |
| 3WYM     | 3K9    | 1,52     | 2ANQ     | NDP    | 2,74     | 5SZ7     | 72H    | 1,92     |
| 4CDL     | LLK    | 4,22     | 2BU5     | TF1    | 3,17     | 6AAH     | 9T6    | 1,78     |
| 4IU6     | FZ1    | 6,34     | 2CL5     | SAM    | 1,95     | 6DND     | PLP    | 0,77     |
| 4MIK     | JIL    | 0,97     | 2F6V     | SK2    | 1,45     | 6OA3     | MOM    | 3,61     |
| 4MQ4     | 2D5    | 2,45     | 2OGZ     | U1N    | 1,97     | 6Q0Z     | P7V    | 1,91     |
| 4NCM     | 704    | 1,11     | 2QDH     | M2P    | 1,76     | 7TLN     | INC    | 1,97     |
| 4YTF     | 4HZ    | 5,04     | 2R3N     | SCX    | 1,88     | 2V11     | C80    | 1,33     |
| 5AFW     | EDO    | 5,58     | 2RF6     | SO4    | 1,05     | 2GZ8     | F3F    | 1,70     |
| 5FI2     | 5XX    | 5,41     |          |        |          |          |        |          |

**Table 2:** PubChem ID and Binding energy of **S1**, **S2** and **F3F**.

| Compound   | PubChem ID | Binding energy (Kj/mol) |
|------------|------------|-------------------------|
| <b>S1</b>  | 1627998    | -39,22                  |
| <b>S2</b>  | 1892742    | -36,27                  |
| <b>F3F</b> | 2822496    | -15,96                  |

### Docking Calculations and Visual Inspection

The co-crystal ligand **F3F** complexed with M<sup>pro</sup> (PDB ID: **2GZ8**) was chosen as starting structure to search for similar compounds from PubChem. In order to identify new potent M<sup>pro</sup> inhibitors,

1880 analog compounds to this ligand were prepared and docked into the active site using FlexX. The resulting top-ranked 100 compounds were further analyzed by visual inspection in order to eliminate false positive ones which may have high docking score but present a bad surface complementarity or haven't a rational number of interactions with the studied binding sites. Out of these, compounds **S1** and **S2** showed a higher M<sup>pro</sup> inhibitory potency than that of **F3F**, the reference molecule, whose binding energy is -15.96 KJ/mol. Still more remarkably, these two compounds showed highest negative binding

energy of -39.22 KJ/mol and -36.27 KJ/mol respectively, thus indicating their important inhibitory potency against the enzyme (Table 2).

### Poses Analysis

The binding mode of the most promising inhibitors **S1** and **S2** into the M<sup>pro</sup> binding site was predicted using the poses given by FlexX. As shown in Fig. 2, these two molecules cover the entire M<sup>pro</sup> binding cavity as in the case of **F3F**, thus leading to a high inhibitory patency.

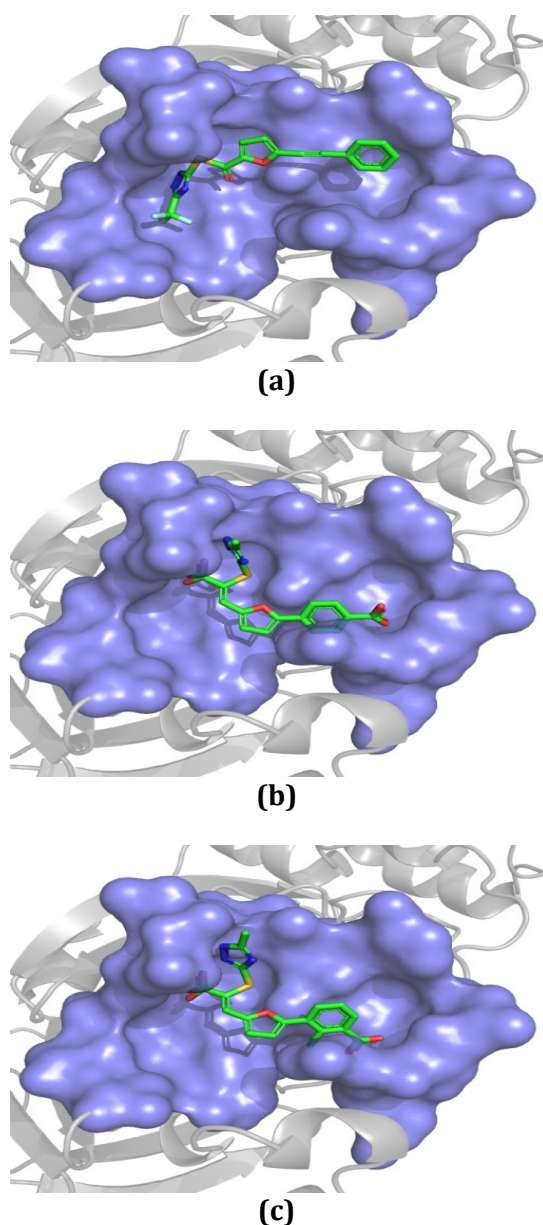


**Figure 2:** Positioning of F3F (a) S1 (b) and S2 (c) into the M<sup>pro</sup> active site. The most plausible pose of each compound is presented as obtained by docking with FlexX. The binding site cavity is represented in blue. The ligand atoms are color-coded as follows: carbon in green, oxygen in red and nitrogen in blue. The images were drawn using PyMol.

The difference of the inhibitory potency between these two promising compounds and **F3F** may be explained by the different number of hydrogen bonds between them and the protein. Indeed, whereas **S1** and **S2** are involved in nine and seven such bonds respectively, **F3F** is involved in only four. In addition, **S1** and **S2** interact with Cys145 in contrary to **F3F** which has a bare contact with this residue. It should be noted that Cys145 was described to play an important role in M<sup>pro</sup> activity because it is one of the catalytic dyad residues in the active site [14].

### Drug Likeness Prediction

Physicochemical, pharmacokinetic and toxicity parameters of **S1**, **S2** and **F3F** were predicted using pkCSM at <http://biosig.unimelb.edu.au/pkcsml/>. As shown in Table 3, **S1** and **S2** had low BBB penetration, which might protect the central nervous system from their potential side effects. They also showed a high gastrointestinal absorption and water solubility, which ensure their further *in vivo* usage.

**Table 3:** The predicted physicochemical, pharmacokinetic and toxicity parameters of **F3F**, **S1** and **S2**.

| Properties                         | F3F      | S1       | S2       |
|------------------------------------|----------|----------|----------|
| Molecular weight                   | 319.87   | 401.50   | 360.79   |
| Rotatable bonds                    | 8        | 8        | 5        |
| H-bond acceptors                   | 2        | 5        | 5        |
| H-bond donors                      | 1        | 2        | 1        |
| Log P                              | 4.15     | 4.10     | 2.80     |
| TPSA Å <sup>2</sup>                | 28.16    | 142.61   | 120.14   |
| Lipinski's rule of 5               | Suitable | Suitable | Suitable |
| Veber's rule                       | Suitable | Suitable | Suitable |
| Water solubility                   | Soluble  | Soluble  | Soluble  |
| GI <sup>[a]</sup> absorption       | High     | High     | High     |
| BBB <sup>[b]</sup> perméabilité    | High     | Low      | Low      |
| CYP <sup>[c]</sup> 1A2 inhibition  | No       | No       | No       |
| CYP <sup>[c]</sup> 2C19 inhibition | No       | No       | No       |
| CYP <sup>[c]</sup> 2C9 inhibition  | No       | No       | No       |
| CYP <sup>[c]</sup> 2D6 inhibition  | No       | No       | No       |
| CYP <sup>[c]</sup> 3A4 inhibition  | No       | No       | No       |
| AMES toxicity                      | Low      | Low      | Low      |
| hERG <sup>[d]</sup> inhibition     | Low      | Low      | Low      |
| Carcinogenicity                    | Low      | Low      | Low      |

[a] GI: Gastro-Intestinal, [b] BBB: Blood-Brain Barrier, [c] CYP: Cytochrome P450, [d] hERG: human ether-ago- go related gene.

Furthermore, they were not found to inhibit CYP (enzymes that should not be inhibited because of their essential role for the metabolism of many drugs in the liver). With no Veber and Lipinski's rule violation, both **S1** and **S2** follow the criteria for orally available drugs. Still more remarkably, they were predicted to be nontoxic according to their negative results for AMES test, hERG inhibition and carcinogenicity.

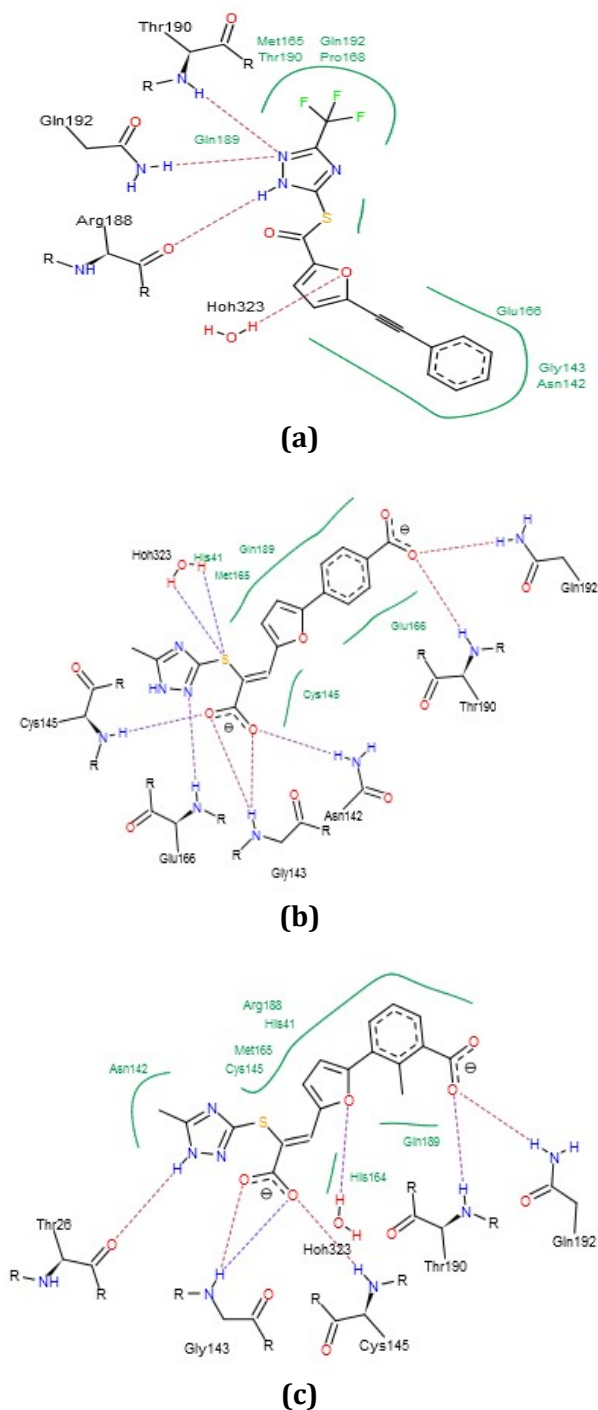


**Figure 3:** Binding mode prediction of **F3F** (a) **S1** (b) and **S2** (c) into the  $M^{pro}$  active pocket. Purple dotted lines represent hydrogen bonds. The images were done with the Ligand Interaction Diagram from LeadIt.

## CONCLUSION

In summary, molecular docking approach was used in order to identify new potent SARS CoV-2  $M^{pro}$  inhibitors. After the validation of docking protocol using RMSD test, compounds **S1** and **S2** were revealed as new inhibitors of this enzyme with binding energy of -39,22 KJ/mol and -36.27 KJ/mol respectively. The binding mode analysis showed that these promising hits cover the entire  $M^{pro}$  binding site in a rational orientation, where their hydrogen bond with Cys145 seem to play an important role, leading to their high inhibitory potency. Still more remarkably, **S1** and **S2** were predicted to have good drug likeness and toxicity profile indicating that they might be promising lead compounds for further anti SARS CoV-2 drug discovery.

## ACKNOWLEDGEMENTS

We are grateful to the Directorate General of Scientific Research and Technological Development, Algeria, for their support.

## HUMAN AND ANIMAL RIGHTS

No Animals/Humans were used for studies that are the basis of this research.

## CONFLICT OF INTEREST

The authors declare no conflict of interest, financial or otherwise.

## ABBREVIATIONS

BBB: Blood-Brain Barrier

COVID-19: Coronavirus disease 2019

CYP: Cytochrome P450

GI: Gastro-Intestinal

hERG: human ether-ago- go related gene

$M^{pro}$ : Main protease

RMSD: Root Mean Square Deviation

SARS-CoV-2: Severe acute respiratory syndrome coronavirus 2

## REFERENCES

- [1] World Health Organization (WHO). Coronavirus Disease (COVID-19) Dashboard. 2022; <https://covid19.who.int/> (Accessed 15/05, 2022).
- [2] Vinayagam S, Sattu K. SARS-CoV-2 and coagulation disorders in different organs. *Life Scien.* 2020; 260: 118431.
- [3] Romagnoli S, Peris A, De Gaudio AR, Geppetti P. SARS-CoV-2 and Covid-19: from the bench to the bedside. *Physiological Revue.* 2020; 100(4): 1455-66.

- [4] Wang D, Hu B, Hu C, Fangfang Z, Xing L, Jing Z et al. Clinical characteristics of 138 hospitalized patients with 2019 novel coronavirus-infected pneumonia in Wuhan, China. *JAMA*. 2020; 323(11): 1061-1069.
- [5] Ullrich S, Nitsche C. The SARS-CoV-2 main protease as drug target. *Bioorganic & Medicinal Chemistry Letters*. 2020; 30 (17): 127377.
- [6] Riddhidev B, Lalith P, Viranga T. Potential SARS-CoV-2 main protease inhibitors. *Drug Discovery Today*. 2021; 26 (3): 804-816.
- [7] Lu IL, Mahindroo N, Liang PH, Peng YH, Kuo CJ, Tsai KC et al. Structure-Based Drug Design and Structural Biology Study of Novel Nonpeptide Inhibitors of Severe Acute Respiratory Syndrome Coronavirus Main Protease. *Journal of Medicinal Chemistry*. 2006; 49: 5154-5161
- [8] "Schrödinger Release 2018-4: LigPrep, Schrödinger, LLC, New York, NY, 2018".
- [9] Lasmari S, Ikhlef S, Boulcina R, Mokrani EH, Bensouici C, Gürbüz N et al. New Silver N-Heterocyclic Carbenes Complexes: Synthesis, Molecular Docking Study and Biological Activities Evaluation as cholinesterase inhibitors and antimicrobials. *Journal of Molecular Structure*. 2021; 1238: 130399.
- [10] Sandeli AK, Khiri-Meribout N, Benzerka S, Gürbüz N, Dünder M, Karcı H et al. Silver (I)-N-heterocyclic carbene complexes: Synthesis and characterization, biological evaluation of Anti-Cholinesterase, anti-alpha-amylase, anti-lipase, and antibacterial activities, and molecular docking study. *Inorganica Chimica Acta*. 2021; 525:120486.
- [11] Boualia I, Derabl C, Boulcina R, Bensouici C, Yildirim M, Yildirim AB et al. Synthesis molecular docking studies, and biological evaluation of novel alkyl bis(4-amino-5-cyanopyrimidine) derivatives. *Archiv der Pharmazie Chemistry in Life Science*. 2019; 325(11): 1-10.
- [12] Rarey M, Kramer B, Lengauer T, Klebe. GA. fast flexible docking method using an incremental construction algorithm. *Journal of Molecular Biology*. 1996; 261: 470-489.
- [13] Mokrani EH, Bensegueni A, Chaput L, Beauvineau C, Djeghim H, Mouawad L. Identification of New Potent Acetylcholinesterase Inhibitors Using Virtual Screening and in vitro Approaches. *Molecular informatics*. 2019; 38(5): 1800118.
- [14] Zeynab F, Shama K, Suliman A, Alkhuriji A, Aijaz A. ABBV-744 as a potential inhibitor of SARS-CoV-2 main protease enzyme against COVID-19. *Scientific Reports*. 2021; 11: 234.
- [15] Belhoula H, Mokrani EH, Bensegueni A, Bioud D. Highlight of New Phosphodiesterase 10A Inhibitors Using Molecular Docking. *Current Research in Bioinformatics*. 2020; 8(1): 34-37.
- [16] Hioal KS, Chikhi A, Bensegueni A, Merzoug A, Boucherit H, Teniou S et al. Successful challenge: A key step in infectious diseases treatment using computer-aided drug design. *International Journal of Biological Science*. 2014; 1(1): 11-14.